Biophysical Chemistry 3 (1975) 297–306

PARTIAL CHARACTERIZATION OF THE 1-ANILINO-8-NAPHTHALENE SULFONATE–ADRENOCHROME SEMICARBAZIDE INTERACTION SITE IN ERYTHROCYTE GHOST MEMBRANE FRAGMENTS*

David B. MILLAR

Laboratory of Physical Biochemistry, Environmental Biosciences Department, Naval Medical Research Institute, National Naval Medical Center, Bethesda, Maryland 20014, USA

and

Colin F. CHIGNELL

Section on Molecular Pharmacology, Pulmonary Branch, National Heart and Lung Institute, National Institutes of Health, Bethesda, Maryland 20014, USA

Received 7 April 1975; revised manuscript received 14 May 1975

The effect of adrenochrome semicarbazide on the conformation of erythrocyte ghost membranes has been studied by ANS fluorescence, lipid and sulfhydryl spin labels and circular dichroism. No large conformational alterations in the membrane were detected by these techniques. Noncompetitive quenching of ANS fluorescence by ADCS suggests ADCS to interact with the membrane at sites close to the ANS binding domain.

1. Introduction

Certain musculoskeletal traumatic injuries have been observed to lead to a hemolytic process known as chronic anemia of trauma. Although the precise mechanism of hemolysis is at present unknown it has been suggested that adrenochrome, and perhaps additional serum factors, may be involved [1]. If adrenochrome is indeed the causative agent, then it seems reasonable to postulate that the interaction of this metabolite with the erythrocyte membrane may ultimately lead to disruption of the membrane continuum and lysis of the cell. The fluorescent probe 1-anilino-8-naphthalene sulfonic acid has been successfully used to study environmental effects on the erythrocyte ghost membrane [2–5]. We have therefore used this label to investigate the influence of adrenochrome on erythrocyte membranes. Spin labels have also been used to study the effects of various perturbing agents, such as drugs [6], benzyl alcohol [7], and azoester [8], on both natural and synthetic membrane systems. Spin-labeled analogs of N-ethylmaleimide (I), iodoacetamide (II), and stearic acid (III) were therefore also used to probe the effect of adrenochrome on ghost membranes. Finally, since circular dichroism measurements of membranes can provide information on the conformation of membrane protein [9], this technique was also used to study the interaction of adrenochrome with ghost membranes.

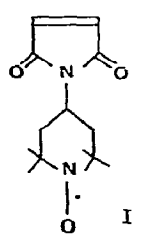

I

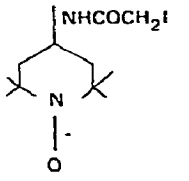

II

* From the Bureau of Medicine and Surgery, Navy Department Research Subtask MF51.524.014.9025. The opinions and statements contained herein are the private ones of the authors and are not to be construed as official or reflecting the views of the Navy Department or the naval service at large.

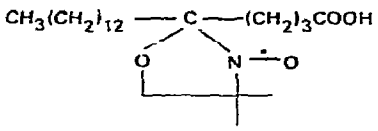

III

2. Materials and methods

Erythrocyte ghosts were prepared from outdated blood bank blood by the method of Dodge et al. [10]. Ghost preparations were repeatedly washed and dialysed [1] until hemoglobin was spectrophotometrically undetectable. Such preparations were routinely stored frozen in 0.01 M sodium phosphate buffer (pH 7.1) at a protein concentration of approximately 20 mg/ml. Membrane protein was measured by the method of Lees and Paxman [11]. Prior to use, ghosts were thawed, diluted to 4 mg/ml with 0.01 M sodium phosphate (pH 7.1) and sonicated using the sonifier apparatus and precautions described previously [12]. Sonication was carried out in an ice bath for two thirty second periods with a two minute rest between sonications at an intensity setting of 65. Ghosts were disrupted in this manner to reduce light scattering anomalies in subsequent optical measurements. Preparations were kept at 4°C and used within two days of sonication since increasing turbidity after this period indicated aggregation. ADCS, purchased from Calbiochem, was used instead of adrenochrome because of its greater stability*.

Fluorescence titrations were performed at 25°C in a thermostatted Aminco–Bowman uncompensated fluorometer having a 15 nanometer bandpass. Polarization of fluorescence was measured in another Aminco–Bowman fluorometer equipped with polacoat polarizing filters. The exciting light was polarized and polarization, P, was calculated from the equation

$$P = (I_{V_1V_2} - GI_{V_1H_2})/(I_{V_1V_2} + GI_{V_1H_2}) , \qquad (1)$$

where 1 and 2 represent the exciting and emitting polarizers, V and H represent vertical and horizontal polarization orientations respectively. G is a correction factor for polarization anomalies introduced by the gratings and is defined as:

$$G = I_{H_1V_2}/I_{H_1H_2} . \qquad (2)$$

G was determined for each polarization experiment. In calculating P, the vertically and horizontally polarized light intensities of a solution of sonicated ghosts and ANS (2X recrystallized) were corrected for particle scattering of the incident light by subtracting the appropriate intensities measured on a sonicated ghost solution without ANS. In several experiments with different preparations the correction ranged from 8 percent to 20 percent of the fluorescence of a membrane-ANS mixture. The calculated polarizations, however, agreed within a mean error of four percent. P_0, the polarization value when no macromolecule rotation occurs during the lifetime of the excited state of the dye, was obtained from a plot of $1/P$ versus T/η (T is absolute temperature, η is viscosity). The values of T/η were obtained by varying solution temperature. The wavelengths chosen for excitation and emission (320 and 500 nm respectively) were selected to approximate the peak transmission of the filters used in estimating the fluorescent lifetime of ANS. τ, the excited state lifetime of ANS, was measured either on a TRW Model 31A nanosecond spectral source and Model 32A decay time computer or in an ORTEC 9200 system. We have assumed a single lifetime for ANS bound to sonicated ghost membranes. The very large number of ANS binding sites probably means the values we observe are averages. Such a possibility does not affect the conclusions of this paper. Corning No. 9863 and 3391 filters were employed to isolate the excitation and emission bands respectively. Addition of dye and of adrenochrome semicarbazide to 10 mm^2 quartz cuvettes was made with Hamilton microsyringes fitted with constant delivery adaptors. Mixing was accomplished by means of a magnetic stirring bar placed in the cuvette. Temperature was monitored by means of a calibrated Yellow Springs Instrument probe. All fluorescence titrations were corrected for dilution and light scattering. All fluorescence intensities were measured as the ratio of the experimental emission to the emission of a sealed cuvette containing ANS in 50% alcohol. In experiments in which ADCS was present, the decrease in excitation beam intensity due to ADCS absorption and consequent ANS emission decrease was corrected for by

* Abbreviations: ADCS, adrenochrome semicarbazide; ANS, 1-anilino-8-naphthalene sulfonic acid.

the method of Parker and Barnes [13] as follows:

$$F_0 = F \times 2.303 D(x_2 - x_1)/(10^{-Dx_1} - 10^{-Dx_2}), \quad (3)$$

where F is fluorescence observed in the presence of ADCS absorbance, D, and x_1 and x_2 are the x-axis dimensions of the rectangle viewed by the phototube, and Dx_1 and Dx_2 are the absorbances at these points. No correction is necessary for ADCS absorption at 485 nm since ADCS displays no absorbance at this wavelength. The correction factors obtained by this equation were experimentally verified by placing a cuvette containing ADCS flush against the entrance slit. The correction factor (f) was calculated from the following equation:

$$f = 0.5(r-1) + 1,$$

where r is the ratio of the emission intensity in the presence and absence of ADCS. A plot of calculated versus observed correction factor had a correlation coefficient of 0.999. This experiment showed the correction factor to be valid to at least 32×10^{-5} M ADCS ($A_{265} = 1.09_6$). This ADCS concentration is twice that attained in the ANS titrations.

The fluorescence data from ANS titrations of sonicated ghosts were analyzed using

$$\frac{1}{F} = \frac{1}{F_{max}} + \frac{K_{1,d}}{L_1 F_{max}}, \quad (4)$$

where L_1 is the total ligand (ANS) concentration, $K_{1,d}$ is the apparent ligand-complex dissociation constant. F_{max} is the fluorescence observed when all ligand sites are occupied. Using the identical assumption employed in deriving eq. (4), the relations expressed in eqs. (5) and (6) are obtained describing the cases in which another ligand (L_2) either competes directly at the primary ligand site (competitive quenching) or binds at another spatially distant site which by some means changes the luminescent behavior of the primary ligand. Such changes could occur by energy transfer or binding site conformational transitions which place the primary ligand in an environment which alters fluorescence.

Competitive quenching:

$$\frac{1}{F} = \frac{K_{1,d}}{F_{max} L_1}\left(1 + \frac{L_2}{K_{2,d}}\right) + \frac{1}{F_{max}}, \quad (5)$$

in which $K_{2,d}$ is the dissociation constant of L_2 from the complex.

Binding at a spatially distant site (non-competitive quenching):

$$\frac{1}{F} = \left(1 + \frac{L_2}{K_{2,d}}\right)\left[\frac{1}{F_{max}} + \left(\frac{K_{1,d}}{F_{max}}\right)\frac{1}{L_1}\right]. \quad (6)$$

Plots of $1/F$ observed versus 1/ligand have the following characteristics:

(a) Only L_1 present:

$$\text{slope} = \frac{K_{1,d}}{F_{max}}, \quad \text{intercept} = \frac{1}{F_{max}}.$$

(b) L_2 acting as a competitive quencher:

$$\text{slope} = \left[1 + \left(\frac{L_2}{K_{2,d}}\right)\right]\frac{K_{1,d}}{F_{max}}, \quad \text{intercept} = \frac{1}{F_{max}}.$$

(c) L_2 acting at a spatially distant site:

$$\text{slope} = \left[1 + \left(\frac{L_2}{K_{2,d}}\right)\right]\frac{K_{1,d}}{F_{max}},$$

$$\text{intercept} = \left[1 + \left(\frac{L_2}{K_{2,d}}\right)\right]\left(\frac{1}{F_{max}}\right).$$

Measurements of the association constant of the complex in the excited state configuration were made using the approach of Weber et al. [14]. In this method the rate of quenching collisions (k_t^*) is given by the expression

$$k_t^* = (1/\tau^1 + 1/\tau^0)/[Q], \quad (7)$$

where τ^1 and τ^0 are the observed fluorescence lifetimes in the presence and absence of quencher (Q) respectively. The fraction of dissociated complex, α, is given by:

$$\alpha = q^1/[q^0(1 + k_t^* \tau^0)], \quad (8)$$

q^1 and q^0 being the fluorescent emission in the presence and absence of quencher. Since

$$\alpha = \frac{C_f}{C_f + QC} \quad \text{and} \quad K_a = \frac{QC}{(C_f)(Q_f)}, \quad (9)$$

where C_f = concentration of ligand, Q_f = concentra-

tion of free quencher, QC = concentration of complex, it follows that

$$K_a = (\alpha^{-1} - 1)(Q_f^{-1}) , \quad (10)$$

and if $Q_{total} \gg C_{total}$ then $Q_f \approx Q_{total}$.

Electron spin resonance (ESR) spectra were recorded at 25°C with a Varian E-4 spectrometer operating at 6.5 GHz. Samples were placed in the cavity in quartz aqueous sample cells (Varian E-248).

Circular dichroism measurements (200–500 nm) were made at 27°C with a Cary 6001 attachment to the Cary 60 spectropolarimeter. Quartz sample cells (Opticell) with 10 mm pathlengths were employed. Final concentrations were erythrocyte ghosts, 0.05 mg protein/ml and sodium phosphate buffer (pH 7.4), 0.01 M.

Erythrocyte ghost membranes (2 mg/ml) or sonicated erythrocyte ghost membranes were reacted with spin labels I or II (10^{-4} M) at 4°C overnight. Unreacted spin label was removed by centrifugation (*10 000 g*) and resuspension in buffer. Washing was repeated four times. This was followed by overnight dialysis at 4°C. Erythrocyte ghost membranes were labeled with stearic acid probe III by the addition of a methanolic solution (2×10^{-3} M) to the membranes. The final concentration of III was 1×10^{-5} M. Molar ellipticity, $[\Theta]_\lambda$, was calculated from the following equation

$$[\Theta]_\lambda = 100 M \Psi_\lambda / Cl ,$$

where M = molecular weight, Ψ_λ = specific ellipticity, C = concentration (gm/liter) and l = pathlength (cm). A mean residue molecular weight of 114 was assumed for the erythrocyte ghost protein [9].

Ultracentrifugation studies employing Schlieren optics were performed at 20°C in the Beckman–Spinco Model E analytical ultracentrifuge. A partial specific volume of 0.75 ml/g was assumed for the sonicated ghost preparations. Absorbtion scans were made on a Cary Model 14M spectrophotometer. All chemicals were the highest purity available. Unless otherwise indicated, all experiments employed 0.01 M sodium phosphate buffer (pH 7.1) at 25°C. Proteins and lipases were purchased from Sigma.

3. Results

3.1. Quenching of ANS ghost membrane fragment fluorescence by ADCS

ANS and ghost membrane fragments (0.4 mg/ml) showed a strong symmetrical fluorescent emission band with an apparent maximum at 485 nm when activated at either 265 nm or 380 nm. This is similar to previously published results with sonicated and intact ghosts [2–5]. Scatchard plot analysis [4] showed about 200 to 300 nmoles of ANS bound/gram of membrane fragment. This is about 10 fold higher than that for nonsonicated ghosts [4]. However, the plots indicated either complex binding or cooperativity. Similar results have been described by Fortes and Hoffman [4] for intact ghosts. Sequential addition of ADCS to such solutions resulted in strong quenching of ANS fluorescence. The relative quenching efficiency of ADCS was found to be, mole for mole, 4×10^3 times greater than KI. The ghost-ANS–ADCS quenching obeyed the linearity requirements of the Stern–Vollmer relationship up to the highest concentration of ADCS employed (16×10^{-5} M).

$$F^0/F = k_q \tau^0 C + 1 , \quad (11a)$$

$$F^0/F = KC + 1 . \quad (11b)$$

In eqs. (11a) and (11b), F^0 is fluorescence in the absence of quencher and F, the fluorescence in the presence of quencher, k_q is the *overall* rate constant for quenching, τ^0 is the fluorescent lifetime in the absence of quencher, and C is the concentration of quencher. Eq. (11b), an alternative form of the Stern–Vollmer relationship, is derived on the basis of a mass action equilibrium approach which describes the formation of a "dark" complex, i.e., a complex which is formed between chromophore and quencher prior to attainment of the excited state and does not fluoresce. In (11b), K is the association constant for such a reaction. Both (11a) and (11b) require linearity if quenching is simple. Assuming only collisional and complex formation pathways, information can be obtained as to the relative contribution of the two pathways by measuring the lifetime of the fluorescent dye, ANS, in the presence and absence of the quencher, ADCS. Pure collisional quenching will strongly decrease the

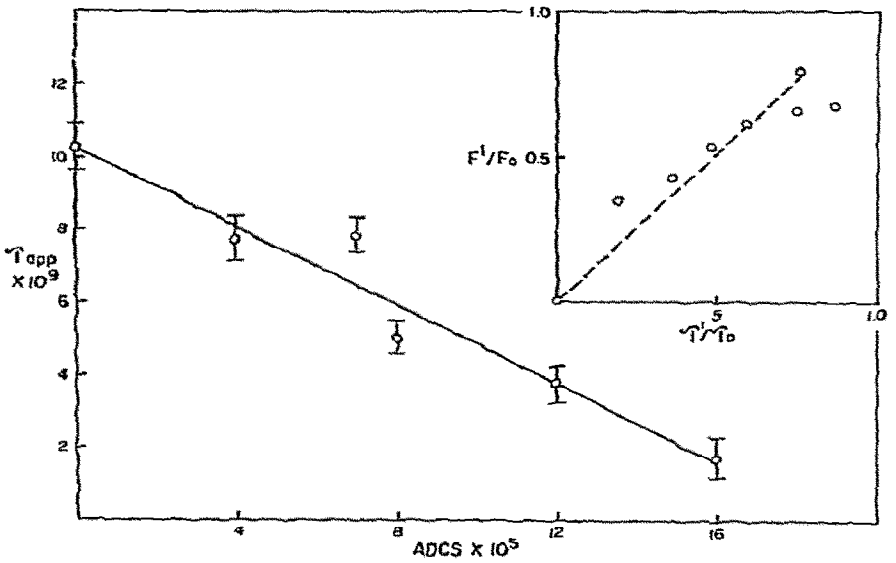

Fig. 1. Affect of varying concentrations ADCS on the lifetime of ANS in the presence of 0.4 mg/ml ghosts. $T = 25°C$. A plot of F^1/F^0 versus τ^1/τ^0. The dotted line is the theoretical line for pure collisional quenching. ANS concentration is in M/l.

measured lifetime while pure "dark" complex formation will not affect it. The results of such measurements are shown in fig. 1. The apparent lifetime falls linearly with increasing ADCS. Weber has pointed out [15] that in pure collisional quenching, the ratio of excited molecules deactivated by emission in the presence, N, and absence, N^0, of quencher should be 1. A plot of F^1/F^0 versus τ^1/τ^0 is shown in the insert in fig. 1. The slope of the plot is N/N^0. The data appear to segregate reasonably close to 1 (dotted line). This analysis suggests collisional interaction between ANS and ADCS on the membrane fragment to be of major importance in the quenching. This interference is lent support by the fact that ADCS quenches ghost-ANS fluorescence approximately 83% as well as it does the fluorescence of ANS in 50% ETOH.

3.2. Apparent size of the ANS–ADCS binding macromolecule

A solution containing 0.4 mg/ml membrane fragments and 2.7×10^{-5} M ANS, was used to estimate the size of the membrane binding site by measuring the temperature dependence of P and estimating P_0 by linear extrapolation of a plot of $1/P$ versus T/η. There was no evidence for label rotational freedom. P_0 was found to be 0.5. Eq. (12) relates these parameters to molecular volume:

$$\frac{1/P-1/3}{1/P_0-1/3} = 1 + \frac{RT\tau}{\eta V}. \qquad (12)$$

In eq. (12), P is polarization, P_0 is the maximal polarization obtained in the absence of macromolecular rotation, R is the gas constant, T is the absolute temperature, V is the molecular volume and η is viscosity. P_{25} was found to be 0.126. For unspecified sonication periods, Freedman and Radda report a P of 0.24 [16]. If it is assumed that the partial specific volume of the membrane protein is 0.75 and that the binding macromolecule is equivalent to a sphere, and that τ does not vary greatly with temperature, the molecular weight of the hydrodynamically equivalent binding unit can be calculated to be approximately ~10 000 daltons. This value could be artificially low if the binding site were associated with a freely rotating polypeptide segment.

Sedimentation velocity analysis showed the ghost membrane preparation to be markedly polydisperse with an average S of 3.2 at a protein concentration of

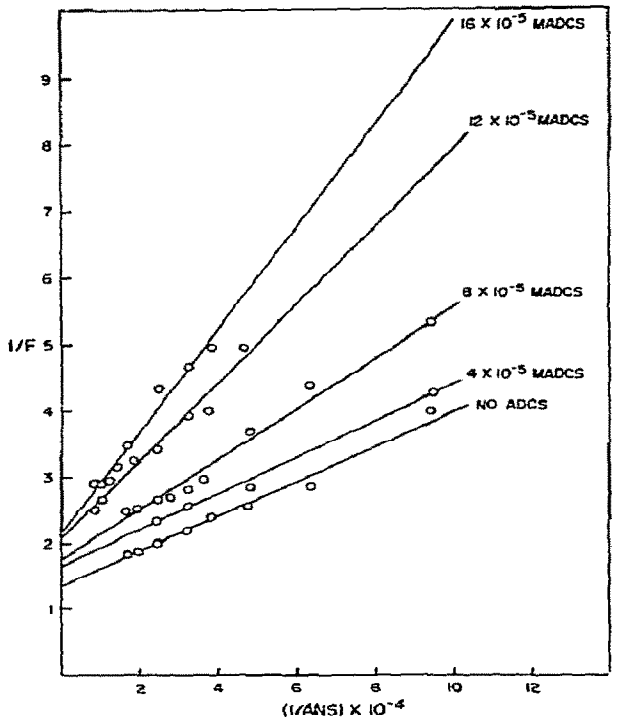

Fig. 2. $1/F$ versus 1/ANS plots in the presence of varying concentrations of ADCS. Ghosts = 0.4 mg/ml. T = 25°C. ANS concentration is in M/ℓ.

2 mg/ml. The molecular weight of the equivalent monodisperse sphere is 30 000. It should be clear that in view of the polydispersity, these molecular weight estimations are order of magnitude values only.

The titration on sonicated erythrocyte ghost preparations with ANS in the presence and absence of ADCS is shown in fig. 2. The results of fig. 2 fit the criteria that ADCS acts as a non-competitive quencher to ANS bound to erythrocyte membrane fragments. The apparent value of $K_{1,d}$ (the membrane fragment–ANS complex) dissociation constant is 2.0×10^{-5} M ± 0.1×10^{-5} (S.D.). For six other preparations studied at this concentration, $K_{1,d}$ has ranged from 5×10^{-5} M to approximately 1.0×10^{-5} M. These values are in good agreement with previous work on sonicated and unsonicated ghosts [2–4]. The average apparent value of the dissociation constant of the membrane fragment–ADCS complex ($K_{2,d}$) was 2.3×10^{-4} M ± 0.5×10^{-4} (S.D.). Using the crude estimates of the molecular weight of the ANS binding site made from the polarization data and the binding data we can calculate that the requirements for the safe use of eq. (10) on the excitation data have been easily met; e.g., at an ADCS level of 4×10^{-5}, and assuming a 1:1 ANS:ADCS competition, the ratio of Q_t to binding sites is 1.5×10^{-3}. The dissociation constants derived from the excited state analysis averaged at 2×10^{-9} ± 0.5×10^{-9}. Such a major shift in apparent K_d can be rationalized with a model wherein the major solvent environment changes occur on or about the excited chromophore affecting the interaction with ADCS.

It is appropriate to point out that plots of $1/F$ versus 1/ligand may be misleading. If it is assumed that only collisional quenching (eq. (11a)) occurs between a quencher and a ligand whose binding is governed by eq. (4), it is possible to compute data which obey the Stern–Vollmer criteria and appear, in plots of $1/F$ versus 1/ligand, to be compatible with non-competitive quenching. Under such circumstances it may become necessary to make both lifetime measurements and independent binding studies in order to be able to define the situation. However, using eqs. (4) and (11b), we have not been able to calculate theoretical data which fits the competitive quenching model. These calculations lend support to the idea that the quenching of ANS fluorescence by ADCS occurs mainly by collisional interaction at or near the ANS binding site.

3.3. Composition of the ANS–ADCS interaction site

To investigate the possibility that erythrocyte membrane protein was important in the quenching phenomena, sonicated ghosts were incubated with the following proteases: trypsin, chymotrypsin, pepsin and pronase. Pepsin is not markedly effective, chymotrypsin and trypsin reduced the binding by about 50–55% while pronase treatment virtually eliminates ANS binding (table 1). The protease treated preparations seem to be more sensitive to ADCS quenching than the control. Table 1 also presents the effect of phospholipases A, C, and D on the binding site. Phospholipase C seems to exert a measurable effect while phospholipase D is somewhat less effective. These results suggest that protein–lipid interactions are important in maintaining the ghost membrane fragment ANS–ADCS inter-

Table 1
Effect of proteases[a] and lipases[b] on the ability of sonicated erythrocyte ghosts to bind ANS and ADCS

	% of control ANS fluorescence	$\frac{\text{ANS + ADCS fluorescence}}{\text{ANS fluorescence}} \times 100$
Protease		
Control	100	45.7
Trypsin	45.1	33.6
Chymotrypsin	50.5	24.9
Pepsin	94.0	35.2
Pronase	4.0	too low to measure
Phospholipase		
Control	100	71.0
A	100	78.5
C	89.8	66.4
D	92.1	73.9

a) 2 ml of 0.4 mg/ml sonicated ghosts plus 0.05 mg/ml of protease were incubated 18 hours at 25°C in 0.01 M Na phosphate buffer, pH 7.1. ANS = 5×10^{-5} M, ADCS = 4.8×10^{-5}.
b) 2 ml of 0.4 mg/ml sonicated ghosts plus 0.05 mg/ml of lipase were incubated as above in 0.01 M tris, 0.01 M Na phosphate, 1.25×10^{-3} M $CaCl_2$, pH 7.8. ANS = 2.71×10^{-5}, ADCS = 2.38×10^{-5}.

action. Protein interactions have previously been suggested to be important for intact erythrocyte membrane ANS binding [3,4].

3.4. Localized binding site effects of ADCS binding

The ESR spectra of human erythrocyte ghost membranes labeled with spin label I showed evidence for the presence of two populations of covalently bound spin labels, one of which was more highly immobilized than the other (fig. 3). The highly immobilized population exhibited a maximum hyperfine splitting of 59.5 G. Similar results have been reported by Holmes and Piette [6] and Chignell and Starkweather [8]. Holmes and Piette have suggested that the highly immobilized labels are attached to sulfhydryl groups buried deep inside the membrane and that the mobile labels are attached to surface sulfhydryl groups. Treatment of the membranes with ADCS (10^{-4} M) did not alter the ESR spectrum of human erythrocyte ghosts labeled with I. The ESR spectrum of sonicated human erythrocyte ghosts labeled with I also showed evidence for two populations of bound spin label. However, in contrast to the intact ghost membranes, the sonicated membranes contained only a small population of highly immobilized labels (fig. 3). This observation suggests that, as a result of sonication, membrane sulfhydryl groups that were in the interior membrane have become exposed. No change in the ESR spectrum of sonicated ghost membranes labeled with I was observed on the addition of ADCS (10^{-4} M).

The ultraviolet circular dichroic spectrum of the sonicated ghosts was characteristic of an α-helical protein. The molar ellipticity, [Θ], of the membranes was −3.05 deg cm^2 decimole^{-1} at 208 nm from which it was possible to calculate [18] that approximately 90% of the membrane protein was in an α-helical conformation. While this value is higher than that previously reported by Lenard and Singer for unsonicated ghost membranes [9], it is in agreement with the ESR measurements which indicate that sonication causes a change in the conformation of erythrocyte membrane protein. The addition of ADCS up to a final concentration of 8×10^{-5} M did not alter the circular dichroic spectrum of the ghost membranes.

When the spin-labeled iodoacetamide analog (II) reacted covalently with the erythrocyte ghost membranes, most of the bound labels exhibited a high degree of mobility (fig. 4). There was, however, evidence for a small population of highly immobilized labels. Holmes and Piette have shown [6] that II reacts preferentially with protein sulfhydryls on the surface of the erythrocyte ghost membranes. Treatment

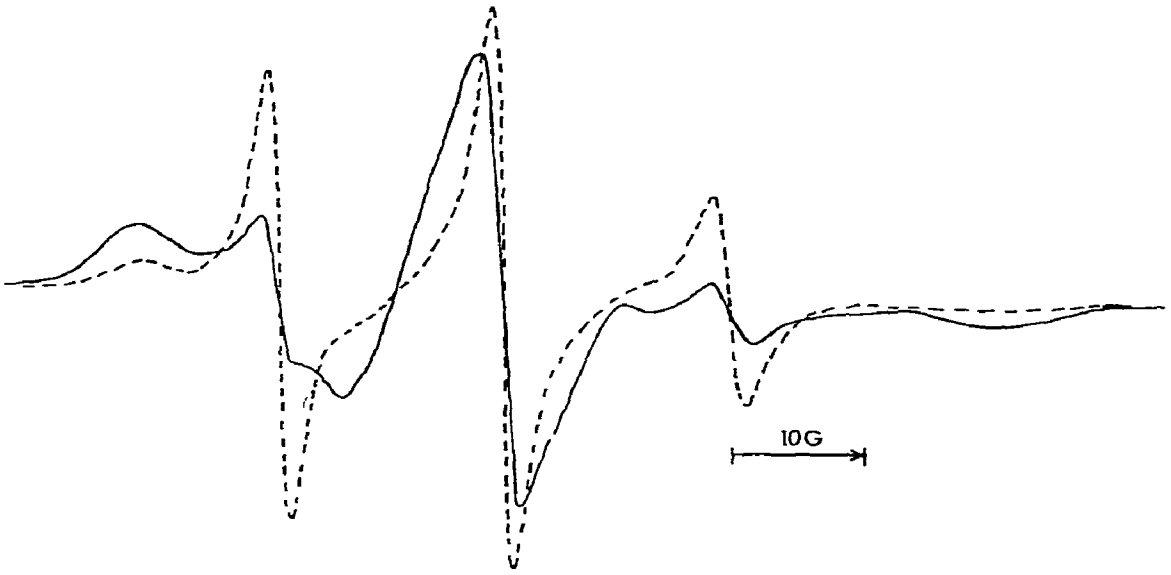

Fig. 3. The ESR spectrum of human erythrocyte ghost membranes (——) and sonicated erythrocyte ghost membranes (- - - -) labeled with I.

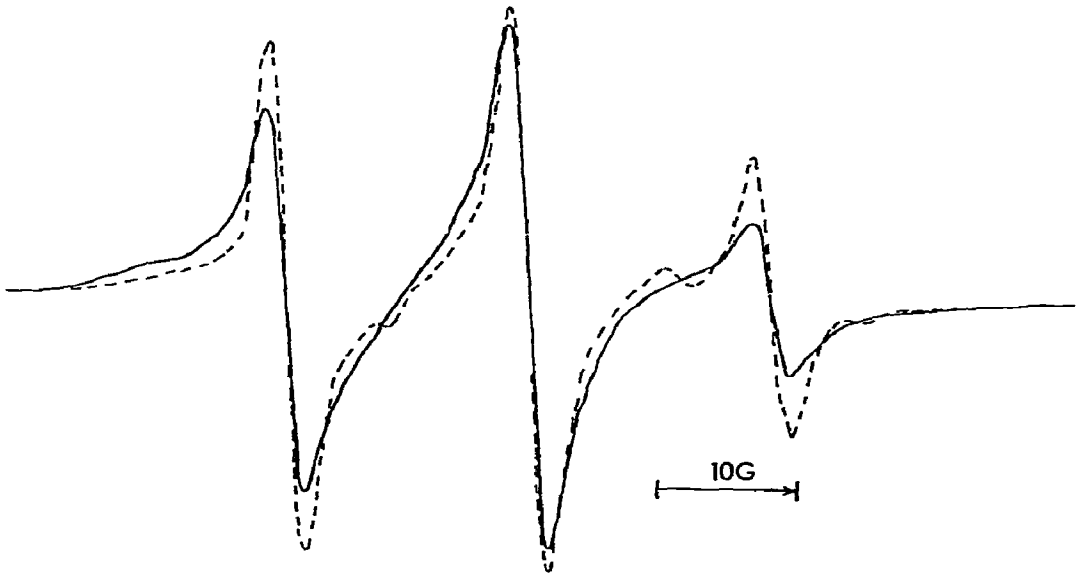

Fig. 4. The ESR spectrum of human erythrocyte ghost membranes (——) and sonicated erythrocyte ghost membranes (- - - -) labeled with II.

of these spin labeled membranes with ADCS (10^{-4} M) did not alter the ESR spectrum of the membranes. Sonication of the human erythrocyte ghost membranes almost completely abolished the highly immobilized population of bound spin label II (fig. 4). The ESR spectrum of the sonicated membranes did not change on the addition of ADCS (10^{-4} M). The CD observations and ESR observations are in harmony and suggest that ADCS does not change any gross change in the protein conformation of either intact or sonicated ghost membranes.

The effect of ADCS on the organization of the lipid in the human erythrocyte ghost membrane was probed with the aid of the stearic acid label (III). In the presence of the ghost membranes, the ESR spectrum of III was that of a highly immobilized nitroxide group with a maximum hyperfine splitting of 65.7 G [17]. Treatment of the membranes with ADCS (10^{-4} M) did not alter the ESR spectrum of III bound to the ghost membranes. Thus it would appear that ADCS does not affect lipid organization in human erythrocyte ghost membranes.

Evidence that there might be a highly localized but small effect of ADCS on the membrane fragment was sought by analysing the data of fig. 2 for the Hill coefficient. The plots of $\log(F/F_{max}-F)$ versus $\log$ (ANS) from which the Hill coefficients were derived were in all cases linear with correlation coefficients of 0.9 or better. The Hill coefficients progressively changed from 0.7 (0 ADCS) to 0.4 (16×10^{-5} ADCS). These results suggest an interaction phenomenon incorporating negative cooperativity. This point is consistent with the Scatchard plots for ANS binding seen previously [4] and with those presented earlier in this report. However, simple noncompetitive or competitive binding should show an invariant Hill coefficient of 1. The change seen here may signal slight cooperative effects in the binding effects too slight to be detected in the unsophisticated analysis used to obtain the data of fig. 2.

4. Conclusion and discussion

The significant results of this investigation are that in the presence of ADCS no detectable alterations occurred in either the protein α-helical structure of the membrane fragments or the membrane internal viscosity; that ADCS is not tightly bound; that the ANS–ADCS binding site depends upon the integrity of both peptide and lipid bonds; and finally that there may be weak and highly localized effects of ADCS in the ANS binding site. Furthermore, since ADCS efficiently quenches the bound ANS fluorescence by a collisional interaction, the ANS, which is presumably located in a surface "pocket" or moderately penetrating into the lipid bilayer, must still have considerable solvent accessibility. This model is supported by the fact that ADCS is 83% as efficient in quenching ANS-ghost emission as it is in quenching ANS in alcohol. As ANS is only minimally fluorescent in water, the membrane fragment binding site must possess some special environment features which permit fluorescence to occur. This point has been considered before for intact ghosts but no convergent viewpoint has emerged [2,3,9]. One possible explanation for the present results is that binding of ANS results in partial immobilization of the ANS and alteration of its rotational, vibrational and configurational freedom so that the quenching solvent conformation present in bulk solvent cannot be attained.

The inability of ADCS to cause a major change in the molecular organization of human erythrocyte ghosts suggests that the hemolytic action of adrenochrome is not simply the direct result of membrane binding but may involve either additional serum born factors and/or a time dependent series of changes in the conformation of the membrane.

Acknowledgement

The authors are grateful to T. Mallinson for expert technical assistance and to Drs. R.L. MacKenzie and R.F. Steiner for their critical comments.

References

[1] C.R. Valeri, M.D. Altschule and L.E. Pivacek, J. Med. 3 (1972) 20–40.
[2] B. Rubalcava, D. Martínez de Muñoz and C. Gitler, Biochem. 8 (1969) 2742–2747.
[3] D.F.H. Wallach, E. Ferber, D. Selin, E. Weidekamm and H. Fischer, Biochim. Biophys. Acta 203 (1970) 67–76.
[4] P.A.G. Fortes and J.F. Hoffman, J. Membrane Biol. 5 (1971) 154–168.

[5] G. Wiethold, D. Hellenbrecht, B. Lemmer and D. Palm, Biochem. Pharmacol. 22 (1973) 1437–1449.
[6] D.E. Holmes and L.H. Piette, J. Pharmacol. Exp. Ther. 173 (1970) 78–84.
[7] W.L. Hubbell, J.C. Metcalfe, S.M. Metcalfe and H.M. McConnell, Biochim. Biophys. Acta 219 (1970) 415–427.
[8] C.F. Chignell and D.K. Starkweather, Life Sci. 14 (1974) 641–652.
[9] J. Lenard and S.J. Singer, Proc. Nat. Acad. Sci. USA 56 (1966) 1828–1835.
[10] J.T. Dodge, C. Mitchell and D.J. Hanahan, Arch Biochem. 100 (1963) 119–130.
[11] M.B. Lees and S. Paxman, Anal. Biochem. 47 (1972) 184–192.
[12] M. MacKenzie and D.B. Millar, Anal. Biochem. 48 (1972) 225–232.
[13] C.A. Parker and W.J. Barnes, Analyst 82 (1957) 606–609.
[14] G. Weber, F. Tanaka, B.Y. Okamoto and H.G. Drickamer, Proc. Nat. Acad. Sci. USA 71 (1974) 1264–1266.
[15] G. Weber, Trans. Faraday Soc. 44 (1948) 185–188.
[16] R.B. Freedman and G.K. Radda, Febs Letters 3 (1969) 150–152.
[17] F.R. Landsberger, J. Paxton and J. Lenard, Biochim. Biophys. Acta 266 (1972) 1–6.
[18] N. Greenfield and G.D. Pasman, Biochem. 8 (1969) 4108–4116.